The 8th Pacific Rim International Congress on Advanced Materials and Processing
Edited by: Fernand Marquis
TMS (The Minerals, Metals & Materials Society), 2013

HEAT TREATMENT EFFECTS ON THE HIGH TEMPERATURE MECHANICAL BEHAVIOR OF DIRECTIONALLY SOLIDIFIED MAR-M247 SUPERALLOY

Hui-Yun Bor[1], Chao-Nan Wei[1], An-Chou Yeh[2],Wei-Bin He[3], Huei-SenWang[3], Chen-Ming Kuo[4]

[1]Materials and Electro-Optics Research Division, Chung-Shan Institute of Science and Technology; P.O. Box 90008-8-4; Lungtan, Taoyuan, 32599, Taiwan
[2]Department of Materials Science and Engineering, National Tsing Hua University; 101, Sec. 2, Kuang-Fu Rd.; Hsinchu, 30013, Taiwan
[3]Department of Materials Science and Engineering, I-Shou University; 1 Sec. 1, Syuecheng Rd.; Dashu, Kaohsiung, 84001, Taiwan
[4]Department of Mechanical and Automation Engineering; 1 Sec. 1, Syuecheng Rd.; Dashu, Kaohsiung, 84001, Taiwan

Keywords: MAR-M247 Superalloy, Directional solidification, Heat treatment, Creep, Tensile

Abstract

In this study, two heat treatment schemes were proposed to study the high temperature mechanical behavior of directionally solidified MAR-M247 superalloy with withdraw rate of 180 mm/h. Standard heat treatment (HT1) procedures are solution treatment at 1230°C for 2 h/GFQ, then first aging at 980°C for 5 h/AC and followed by second aging at 870°C for 20 h/AC. Modified heat treatment (HT2) is solution treatment at 1260°C for 3 h/GFQ and first aging at 980°C for 6 h/AC, then the same second aging procedure. Uneven size and shape of gamma prime precipitates are observed after full HT1 scheme, whereas even size but fusion-alike gamma prime precipitates are observed in HT2 specimen. Creep tests at high temperature/low stress (982°C/200MPa) conditions show similar creep rupture life but low extension rate of HT1 specimen. Uneven size and shape of gamma prime precipitates of HT1 specimen effectively prevent dislocation motion. However, the yield strength, tensile strength and elongation to failure of HT2 specimens at 982°C are higher than these of HT1 specimens.

Introduction

Gas turbine blades used for engines in sea, land and air are mostly made of nickel-based superalloys [1,2]. These alloys are strengthened through the precipitation of γ' phase, $Ni_3(Al, Ti)$, in a γ-Ni matrix. This precipitation phase provides good mechanical properties, such as creep resistance at high temperatures [2]. The size, morphology and volume fraction of γ' particles have been shown to affect the mechanical properties of superalloys [3-6]. Solution heat-treatments are common in nickel-based superalloys and play a key role for the application of these materials at high temperatures [7-9]. The objectives of this heat-treatment are the complete solutioning of γ' phase in the γ matrix and minimizing the segregation from non-equilibrium solidification in preparation for the aging heat-treatment [10]. After solution treatment, aging treatments are performed to generate uniform distribution precipitations.

MAR-M247 is a typical polycrystalline/directionally solidified (DS) nickel-based superalloy applied in investment casting, which was developed by Danesi et al. at the Martin Company in the 1970's [11]. Its optimal alloy design and microstructural control make the MAR-M247 superalloy highly castable and very strong in high temperature. Besides, it also exhibits excellent resistance to creep and hot corrosion [12-15]. According to the literature, that after heat treatment, the volume percentage of the γ'-phase reaches 62% [16]. It's a precipitation hardening type of Nickel-base superalloy. Due to good creep resistance and high oxidation resistance in high temperature environment, MAR-M247 superalloy widely used in the past twenty years in the engine industries [17]. The polycrystalline casting is poor mechanical properties at high temperatures, therefore, in recent years the development of high-temperature alloys vast majority concentrated not only in the alloy design but also directional solidification and single-crystal processes. Its purpose is to improve the engine operating temperature, enhance the efficiency of the engine and thrust. When the directional solidification in the [001] crystalline orientation is designed as the main axis parallel to the blade in the superalloy, it can improve the mechanical strength [18].

In this study, directionally solidified MAR-M247 superalloy specimens were prepared, then by the use of different heat treatment schemes to alternate γ' size and its morphology. In high temperature mechanical property measurements, creep test at 982°C/200MPa as well as tensile test at 25°C and 982°C were conducted. Microstructure and composition analysis were observed and measured by the use of scanning electron microscope (SEM) and energy dispersive spectrometer (EDS), respectively. Correlations between observed microstructures and high temperature mechanical properties were investigated.

Experiments

The chemical composition of MAR-M247 superalloy used in this work is given in Table I. The 12 mm diameter DS MAR-M247 specimens were cast under Bridgeman type furnace with a withdrawal rate of 180 mm/hr. DS specimens were subjected to two different heat treatment schemes: (HT1) solution treatment at 1230°C for 2h + 1st aging at 980°C for 5h + 2nd aging at 870°C for 20h, (HT2) solution treatment at 1260°C for 3h + 1st aging at 980°C for 6h + 2nd aging at 870°C for 20h. After solution treatment, argon cooling was performed; air cooling was used after each aging treatment.

Table I. Chemical composition of Mar-M247 superalloy in wt.%.

	Ni	W	Co	Cr	Al	Ta	Hf	Ti	Mo	C	B	Zr
Mar-M247	bal.	10	10	8.3	5.5	3.0	1.5	1.0	0.7	0.15	0.015	0.050

DS round bars were machined into 6.35 mm diameter and 25.4 mm gage length creep test specimens. Creep tests were performed at 982°C/200MPa with a lever arm creep tester ATS Series 2330. Three thermocouples were attached to the gage length of each specimen and were controlled within ±0.1°C during all creep tests. Tensile test were carried out in air at 25°C and 982°C. Cylindrical specimens of 6.25 mm diameter and 34 mm gage length were employed for tensile test. Tensile machine was MTS high temperature servohydralic material test system.

The microstructures of the specimens were examined on Hitachi-4700 and Hitachi-3400 SEM. The system is equipped with a Horiba EDS system, which was used to semi-quantitatively measure the chemical composition of precipitates. Samples for SEM microscopy were prepared metallographically and etched by phosphoric acid (70ml H_3PO_4 + 30ml H_2O).

Results and Discussion

Microstructure Analysis

Figure 1(a) shows the macroscopic observation of as-cast DS bar with grain size around 2.5 mm to 5 mm. The γ' precipitate of as-cast DS specimen is a cuboidal shape as shown in Figure 1(b). After heat treatment, the size, shape and distribution of γ′ particles in the DS specimens under HT1 and HT2 conditions are displayed in Figures 2(a) and 2(b), respectively. HT1 results in uneven distribution of the γ′ precipitates, 0.5 to 0.7 μm as the larger ones whereas 0.1 to 0.4 μm as the smaller ones. As HT2, the γ′ precipitate is around 0.1 to 0.4 μm in size and uniformly distributed in the matrix. There exist a large number of eutectic phases in both grains and grain boundaries after HT1. Both γ′/γ eutectic and MC type carbide are observed inside the grain and at the grain boundary of HT1 specimens as shown in Figure 3, however, a small amount of $M_{23}C_6$ type carbide distributed on the grain boundary is found in Figure 3(b). In HT2 specimens, only MC type carbide is found inside the grain and at the grain boundaries as shown in Figure 4. It is also found that a small amount of the $M_{23}C_6$ carbide at the grain boundaries as shown in Figure 4(b). $M_{23}C_6$ carbide is usually precipitated along the grain boundaries in the aging process and increases the mechanical strength. In order to improve the mechanical properties, not only solid solution and aging heat treatment to improve the γ′ phase in the volume fraction of the substrate, but also $M_{23}C_6$ or M_6C carbides at the grain boundaries are formed [19].

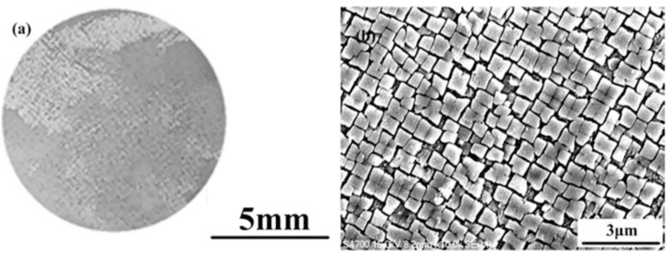

Figure 1. As-cast DS Mar-M247 with 180 mm/hr drawing rate (a) cross-sectional view, (b) microstructure view.

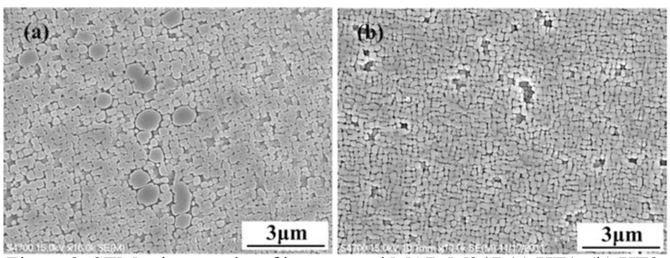

Figure 2. SEM micrographs of heat treated MAR-M247 (a) HT1, (b) HT2.

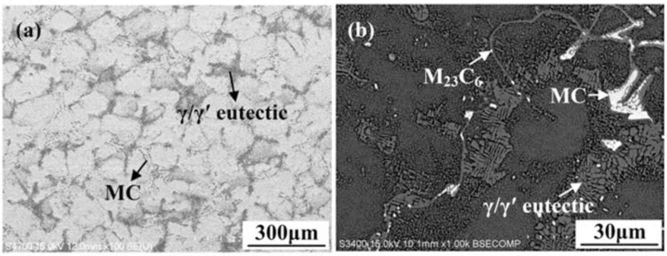

Figure 3. SEM micrographs of HT1 heat treatment of DS MAR-M247 (a) inside the grain, (b) at the grain boundary.

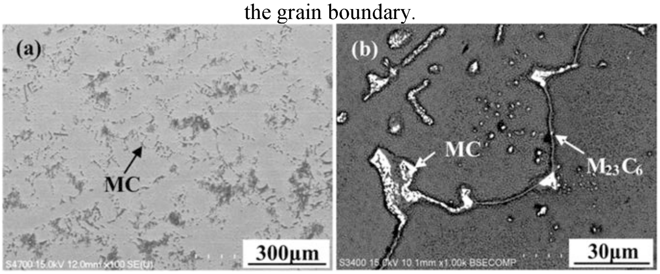

Figure 4. SEM micrographs of HT2 heat treatment of DS MAR-M247 (a)grain, (b)grain boundary.

Creep Test

The creep curves of both HT1 and HT2 are show in Figure 5. The creep rupture life of both HT1 and HT2 are very similar, however, the creep strain of HT2 is almost three times than that of HT1. Due to uneven size of the γ′ precipitate, dislocation movement is effectively obstructed in HT1 specimens. The rafts of γ′ platelets of HT1 and HT2 are shown in Figures 6(a) and 6(b), respectively. Smooth fracture surface of HT1 SEM fractograph, Figure 7(a) suggests brittle fracture as the 6% creep strain. Whereas, dimples are observed in the HT2 SEM fractograph, Figure 7(b), which recommends large plastic deformation during high temperature creep test so as to 18% creep strain. EDS analyses of near fracture surfaces of both HT1 and HT2 crept specimens show MC type carbide near the fracture path, Figure 8. Since the MC carbide is a brittle phase, stress concentration near its surroundings causes fracture.

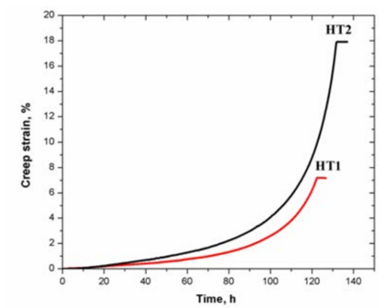

Figure 5. Creep curves of HT1 and HT2 DS MAR-M247 superalloy under 982°C/200MPa.

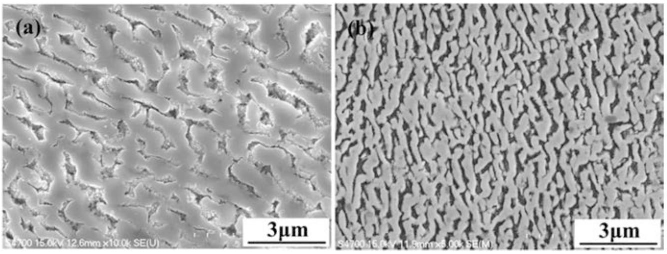

Figure 6. Raft structure of DS MAR-M247 superalloy crept at 982˚C/200MPa (a) HT1, (b) HT2.

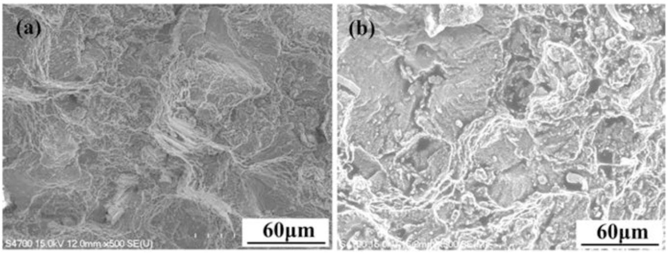

Figure 7. SEM fractographs of DS MAR-M247 superalloy crept at 982˚C/200MPa (a) HT1, (b) HT2.

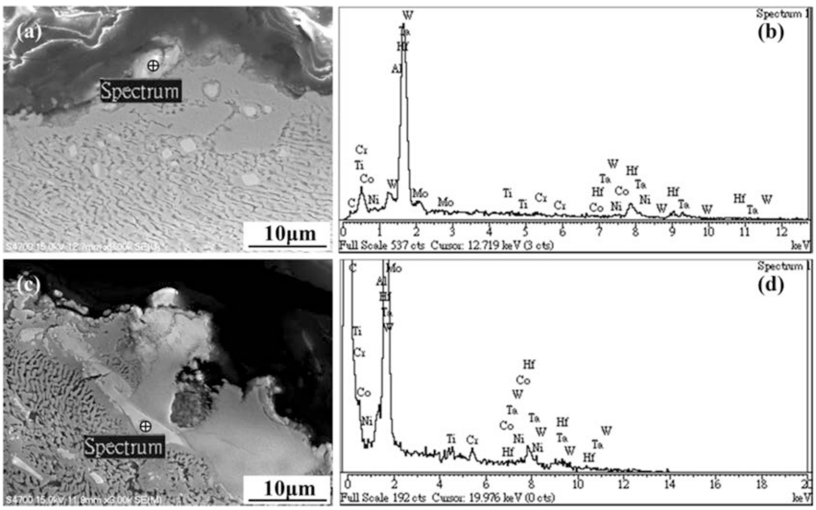

Figure 8. Near fracture surface of DS MAR-M247 superalloy crept at 982˚C/200MPa (a) HT1 and (b) its EDS result; (c) HT2 and (d) its EDS result.

Tensile test

Typical tensile curves of HT1 and HT2 DS MAR-M247 superalloy at 25°C and at 982°C are shown in Figures 9(a) and 9(b), respectively. Comparisons between HT1 and HT2 on the tensile properties, such as elongation to failure, ultimate tensile strength (UTS) and yield strength, are respectively shown in Figures 10(a), 10(b) and 10(c). All three tensile properties of HT2 specimens are higher than these of HT1 specimens either at room temperature 25°C or at high temperature 982°C. SEM fractographs of HT1 and HT2 at 982°C tensile test are shown in Figures 11(a) and 11(b), respectively. Both figures suggest carbides and grain boundary attribute to the fracture path of high temperature tensile test. Uneven distribution of the γ′ precipitates attributes to the initial fracture of HT1 specimen as shown by SEM photo and its EDS analysis in Figures 12(a) and 12(b), respectively. As HT2 specimen, the $M_{23}C_6$ type carbide could be found near fracture surface (Figures 12(c) and 12(d)). The $M_{23}C_6$ type carbide, $(W, Cr)_{23}C_6$ by EDS analysis, could effectively inhibit grain boundary sliding so that both elongation to failure and UTS of HT2 are higher that these of HT1.

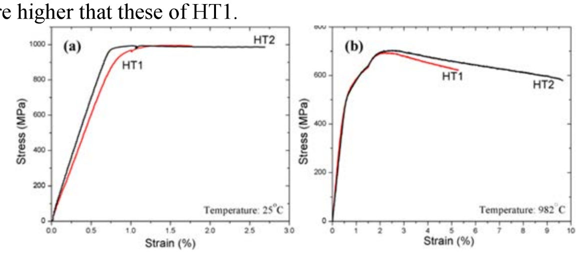

Figure 9. Tensile curves of HT1 and HT2 DS MAR-M247 superalloy (a) at 25°C, (b) at 982°C.

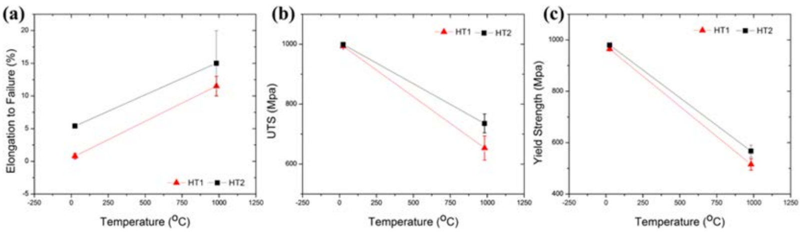

Figure 10. Comparisons between HT1 and HT2 specimens of DS MAR-M247 superalloy on the tensile properties (a) elongation to failure, (b) ultimate tensile strength, (c) yield strength.

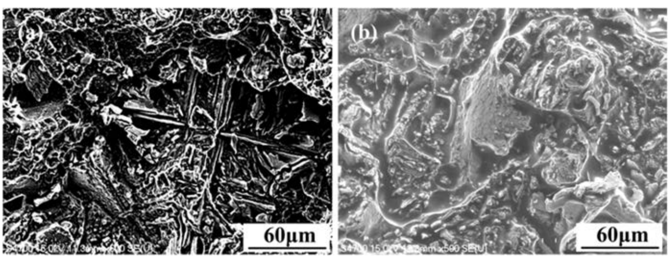

Figure 11. SEM fractographs of DS MAR-M247 superalloy at 982°C tensile test (a) HT1, (b) HT2.

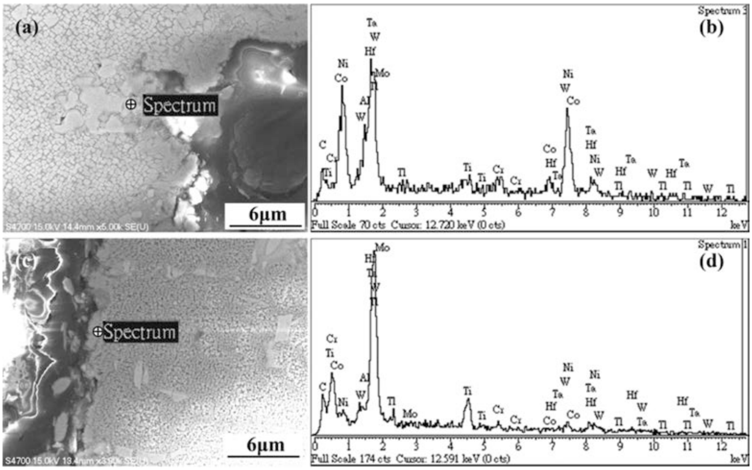

Figure 12. Near fracture surface of DS MAR-M247 superalloy at 982°C tensile test (a) HT1 and (b) its EDS result; (c) HT2 and (d) its EDS result.

Conclusions

In this study, DS MAR-M247 superalloy specimens were prepared to study heat treatment effects on the high temperature mechanical properties. Results are summarized as following:

1. HT1 results in uneven distribution of the γ' precipitates, 0.5 to 0.7 μm as the larger ones whereas 0.1 to 0.4 μm as the smaller ones. As HT2, the γ' precipitate is around 0.1 to 0.4 μm in size and uniformly distributed in the matrix.
2. The creep rupture life under 982°C/200MPa of both HT1 and HT2 are very similar, however, the creep strain of HT2 is almost three times than that of HT1. Due to uneven size of the γ' precipitate, dislocation movement is effectively obstructed in HT1 specimens.
3. All three tensile properties (elongation to failure, UTS and yield strength) of HT2 specimens are higher than these of HT1 specimens either at room temperature 25°C or at high temperature 982°C. Uneven distribution of the γ' precipitates attributes to the initial fracture of HT1 specimens.

Acknowledgements

This work was supported by National Science Council of Taiwan and Chung-Shan Institute of Science and Technology under grant numbers NSC 100-2632-E-214-073-MY3 and XV01D03P004PE, respectively. SEM photographs were conducted at MANA-Laboratory of I-Shou University.

References

1. C. T. Sims, N. S. Stoloff, and W. C. Hagel, *Superalloy II* (New York, NY: John Wiley and Sons, 1987).
2. M. T. Kim, S. Y. Chang, and J. B. Won, "Effect of HIP Process on the Micro-structural Evolution of a Nickel-based Superalloy," *Materials Science and Engineering A*, 441 (2006), 126-134.

3. A. M. Brass, D. Roux, and J. Chene, "Precipitation and Hydrogen on the First Stage of the Plastic Deformation of the Metric of a Ni base Superalloy Single Crystal," *Materials Science and Engineering A*, 323 (2002), 97-102.
4. T. Murakurmo, T. Kobayashi, Y. Koizumi, and H. Harada, "Creep Behavior of Ni-base Single Crystal Superalloy with Various γ' Volume Fraction," *Acta Metall*, 52 (12) (2004), 3737-3744.
5. L. Z. He, Q. Zheng, X. F. Sun, H. R. Guan, Z. Q. Hu, A. K. Tieu, C. Lu, and H. T. Zhu, "Effect of heat treatment on microstructure and tensile properties of Ni-base superalloy M963," *Materials Science and Engineering A*, 398 (1-2) (2005), 128-136.
6. I. M. Wolff, "Precipitation Accompanying Overheating in Nickel-base Superalloy," *Materials Performance*, 29 (2009), 55-62.
7. R. C. Kramb, M. M. Antony, and S. L. Semiatin, "Homogenization of a Nickel-base Superalloy Ingot Material," *Scripta Materials*, 54 (9) (2006), 1645-1649.
8. K. L. Zeisler-Mashl and B. J. Pletka, "Segregation During Solidification in the MAR-M247," *Superalloys 1992*, ed. S.D Antolovich, R.W. Stusrud, R.A. Mackay, D.L. Anton, T. Khan, R.D. Kissinger, and D.L. Klarstrom (Warrendale, PA: The Minerals, Metals & Materials Society, 1992), 175-184.
9. S. R. Hegde, R. M. Kearsey, and J. C. Beddoes, "Designing Homogenization-solution Heat Treatment for Single Crystal Superalloys," *Materials Science and Engineering A*, 527 (21-22) (2010), 5528-5538.
10. G. E. Fuchs, "Solution Heat Treatment Response of a Third Generation Single Crystal Ni-base Superalloy," *Materials Science and Engineering A*, 300 (1-2) (2001), 52-60.
11. H. Y. Bor, C. N. Wei, R. R. Jeng, and P. Y. Ko, "Elucidating the Effects of Solution and Double Ageing Treatment on the Mechanical Properties and Toughness of MAR-M247 Superalloy at High Temperature," *Materials Chemistry and Physics*, 109 (2008), 334-341.
12. J. E. Doherty, B. H. Kear, and A. F. Giamiei, "Origin of Ductility Enhancement in Hf-doped Mar-M200," *J. Metals*, 23 (1) (1971), 59-62.
13. D. N. Duhi and C. P. Sullivan, *J. Metals*, 23 (7) (1971), 38-40.
14. M. V. Nathal, R. D. Maier, and L. J. Ebert, "The Influence of Cobalt on the Tensile and Stress-Rupture Properties of the Nickel-Base Superalloy MAR-M247," *Metallurgical Transactions A*, 13 (1982), 1767-1774.
15. M. V. Nathal, R. D. Maier, and L. J. Ebert, "The Influence of Cobalt on the Microstructure of the Nickel-Base Superalloy MAR-M247," *Metallurgical Transactions A*, 13 (1982), 1775-1783.
16. K. Harris, G. L. Erickson, and R. E. Schwer, "Mar M247 Derivations CM 247 LC DS Alloy CMSX Single Crystal Alloy Properties & Performance," *Superalloy 1984*, ed. M. Gell, C.S. Kortovich, R.H. Bricknell, W.B. Kent, and J.F. Radavich (Warrendale, PA: The Minerals, Metals & Materials Society, 1984), 221-230.
17. H. Y. Bor, C. G. Chao, and C. Y. Ma, "The Influence of Magnesium on Carbide Characteristics and Creep Behavior of the MAR-M247 Superalloy," *Scripta Materials*, 38 (1998), 329-335.
18. K. Harris, G. L. Erickson, and R. E. Schwer, "Development of the CMSX Series of Single Crystal Alloys for Advanced Technology Turbine Components," (Paper presented at TMS-AMIE Fall Meeting, St. Louis, Missouri, 27 October 1982), 1-36.
19. I. S. Kim, B. G. Choi, S. M. Seo, D. H. Kim, and C. Y. Jo, "Influence of Heat Treatment on Microstructure and Tensile Properties of Conventionally Cast and Directionally Solidified Superalloy CM247LC," *Materials Letters*, 62 (6-7) (2008), 1110-1113.